ELSEVIER

Fast-gelling injectable blend of hyaluronan and methylcellulose for intrathecal, localized delivery to the injured spinal cord

Dimpy Gupta[a,b], Charles H. Tator[c], Molly S. Shoichet[a,b,d],*

[a]*Department of Chemical Engineering and Applied Chemistry, University of Toronto, 200 College Street, Toronto, Ont., Canada M5S 3E5*
[b]*Institute of Biomaterials and Biomedical Engineering, 4 Taddle Creek Road, Room 407, Toronto, Ont., Canada M5S 3G9*
[c]*Krembil Neuroscience Centre, Toronto Western Research Institute, and Department of Surgery, University of Toronto, 399 Bathurst Street, Toronto, Ont., Canada M5T 2S8*
[d]*Department of Chemistry, University of Toronto, 80 St. George Street, Toronto, Ont., Canada M5S 3H6*

Abstract

Strategies for spinal cord injury repair are limited, in part, by poor drug delivery techniques. A novel drug delivery system (DDS) is being developed in our laboratory that can provide localized release of growth factors from an injectable gel. The gel must be fast-gelling, non-cell adhesive, degradable, and biocompatible as an injectable intrathecal DDS. A gel that meets these design criteria is a blend of hyaluronan and methylcellulose (HAMC). Unlike other injectable gels, HAMC is already at the gelation point prior to injection. It is injectable due to its shear-thinning property, and its gel strength increases with temperature. In vivo rat studies show that HAMC is biocompatible within the intrathecal space for 1 month, and may provide therapeutic benefit, in terms of behavior, as measured by the Basso, Beattie and Bresnahan (BBB) locomotor scale, and inflammation. These data suggest that HAMC is a promising gel for localized delivery of therapeutic agents to the injured spinal cord.
© 2005 Elsevier Ltd. All rights reserved.

Keywords: Biocompatibility; Injectable; Spinal cord injury; Shear-thinning; Thermally responsive material; Intrathecal

1. Introduction

Of the several therapeutic strategies investigated for spinal cord injury repair [1–3], only systemic delivery of methylprednisolone is used clinically; however, results from its clinical trial have been openly criticized [4]. Other therapeutic strategies that have been investigated hold great promise [5], yet prolonged systemic delivery is notorious for side effects, and the more promising therapeutic proteins degrade when delivered systemically. Moreover, many therapeutic molecules are unable to cross the blood–spinal cord barrier. These difficulties suggest that local delivery strategies are required.

Two intrathecal techniques have been used to test localized delivery: (1) bolus injection, the effects of which are short-lived because the therapeutic is washed away by the cerebrospinal fluid (CSF) flow [6,7] and (2) minipump delivery, which is invasive and can lead to complications of the catheter being blocked and/or infection [8]. A third technique has the therapeutic molecule dispersed in an injectable gel that localizes release to the site of injection. We have previously demonstrated that intrathecal injection of a collagen is safe [9] and can provide localized release of growth factors into the injured spinal cord [10]. However, the collagen gel previously used was not ideal because it was not sufficiently fast-gelling, and caused cellular build-up in the intrathecal space when growth factors were incorporated within [11]. To overcome these limitations, a new injectable gel was required. The design criteria included: (1) fast gelling to ensure delivery would be localized to the site of injection, and that the polymer would not spread with the CSF flow; (2) injectable through

---

*Corresponding author. Department of Chemical Engineering and Applied Chemistry, University of Toronto, 200 College Street, Toronto, Ont., Canada M5S 3E5. Tel.: +1 416 978 1460; fax: +1 416 978 4317.

E-mail address: molly@chem-eng.utoronto.ca (M.S. Shoichet).

a 30G needle to allow for a minimally invasive surgery; (3) non-cell adhesive to minimize the possibility of scar formation in the intrathecal space; (4) degradable to obviate the need for removal after release; and (5) biocompatible to minimize foreign body reaction.

There are several injectable gels that can be described as either physical or chemical gels [12,13]. While both are effective, chemical gels require in situ crosslinking which can involve cytotoxic crosslinkers, free radicals, and/or immobilization of the therapeutic during this reaction. Physical gels, while often not as stable or robust as chemical gels, were investigated for intrathecal injection because "weak" gels were thought to be suitable for this application and the gelation system was simpler, with the use of potentially cytotoxic crosslinking agents obviated. Two physical gels that are known to be generally non-cell adhesive are methylcellulose (MC) and hyaluronan (HA), due, in part, to their hydrophilicity [14].

MC has inverse thermal gelling properties. As the temperature increases, hydrogen bonds between the polymer and surrounding solvent break, and hydrophobic junctions form to produce a gel [15]. MC forms weak gels at 37 °C when in water. The gelation temperature decreases as the salt concentration increases [16] because water molecules surround the salts, thus reducing the solubility of MC in water [17]. Although regenerated cellulose is known to activate the complement system [18], MC has previously shown good biocompatibility when used as scaffolds in traumatic brain injury and peripheral nerve regeneration [19,20]. Inverse thermal gelling polymers such as MC are not sufficiently fast gelling for the injectable drug delivery system (DDS).

HA has found widespread use because it is non-immunogenic and biocompatible [21]. HA is known to promote wound healing by reducing inflammation and minimizing tissue adhesion and scar formation [22]. HA has unique rheological properties [23] because its long polymeric chains form random coils and gel due to molecular entanglements [22]. Under shear force, the molecules align with the direction of stress and flow [24]. However, due to the high water solubility of HA, it quickly disperses when injected into fluid-filled cavities. Few HA derivatives maintain the injectable nature of HA unless mildly crosslinked prior to injection [25].

A fast-gelling, injectable material was created, for the first time, by blending HA and MC (HAMC), and specifically 2% HA with 7% MC. The objectives of this study were to test HAMC against the design criteria, and to better understand its potential for intrathecal delivery. The gelation mechanism, degradation profile, and cell adhesion of HAMC were studied in vitro and the injectability, biocompatibility and therapeutic efficacy were studied in vivo. To better understand the mechanisms of gelation and degradation, the 2% HA/7% MC blend (HAMC) was compared to: 7% MC, 9% MC, and a blend of acetic hydrazide-modified HAMC (acet-HAMC). The acetic hydrazide modification sheds light on the importance of free carboxylic acid groups on HA for HAMC gelation. The biocompatibility of HAMC within the intrathecal space was further examined in vivo in both uninjured and spinal cord injured rat animal models relative to controls of artificial CSF (aCSF) injections.

2. Materials and methods

All media and cells were purchased from ATCC (Rockville, MD) and all reagents were sterile-filtered prior to use. Water was distilled and deionized using Millipore Milli-RO 10 Plus and Milli-Q UF Plus (Bedford, MA) at 18 MΩ resistance. aCSF mimicked the physiologic ion concentrations of the CSF, and consisted of the following: 148 mM NaCl, 3 mM KCl, 0.8 mM $MgCl_2$, 1.4 mM $CaCl_2$, 1.5 mM Na_2HPO_4, 0.2 mM NaH_2PO_4, and 0.1 mg/ml bovine serum albumin [9].

2.1. Preparation of MC, HA and blends

MC A15 PREM LV (Dow Chemical, Michigan, USA) was sterilized by autoclaving for 20 min at 120 °C. MC solutions of 7% (w/w) and 9% (w/w) were prepared in aCSF according to a published procedure [19]. A 0.1 w/v solution of HA (MW 1,500,000, Novamatrix, Norway) in water was sterile-filtered through a 0.22 μm PES filter (Nalgene, Rochester, NY, USA), and lyophilized under sterile conditions. HAMC is a physical blend of 2% HA and 7% MC in aCSF. To produce HAMC, the sterile HA powder was added to the sterile 7% MC solution, vortexed and allowed to dissolve into the MC solution overnight at 4 °C.

HA was modified with acetic hydrazide (Sigma Aldrich, Oakville, ON, CA) using carbodiimide chemistry, a modification previously published [26]. To a 1% HA solution in water, a 2 molar excess of 1-ethyl-3-(3-dimethylaminopropyl) carbodiimide hydrochloride (EDC) (Sigma Aldrich, Oakville, ON, CA) was added at pH 4–4.75, and then a 2 molar excess of acetic hydrazide was added with the pH maintained between 2 and 4.75 by addition of HCl. The solution was stirred overnight and dialyzed using a 10,000 MW cutoff dialysis bag (SpectrumLab, Greensboro, NC, USA) for 2 d in a 10 mM NaCl buffer. The modified HA (acet-HA) solution was sterile-filtered and lyophilized prior to use.

The degree of substitution for acet-HA was determined using ^{1}H-NMR spectroscopy of a 0.1% (w/v) in D_2O using a Gemini 300 spectrometer (Varian). The degree of substitution was calculated by comparing the integrated areas of the methyl derived from the acetic hydrazide moiety of the D-glucuronic acid residues ($\delta = 1.9$ ppm, 3 H) relative to the methyl of the acetamide moiety of the N-acetyl-D-glucosamine residues resonance ($\delta = 2.1$ ppm, 3 H). The degree of substitution was determined to be approximately 80 mol%. Acet-HAMC is a physical blend of 2% acet-HA and 7% MC in aCSF and was prepared as described above for HAMC.

2.2. Gelation time and rheology

Gelation was assessed using the inverted tube test. Two ml microcentrifuge tubes (Fisher Scientific, Ottawa, ON, CA) were filled with 900 μl aCSF and equilibrated to 37 °C. One hundred μl of the polymer solution was injected into the bottom of the tube and incubated at 37 °C. At 2, 5, 10, 15, and 20 min intervals, tubes were inverted to observe if the gel flowed. The time at which the gel did not flow was recorded as the gelation time.

Rheological evaluation was performed on an AR1000 (TA Instruments, New Castle, DE, USA) using a cone and plate geometry, with cone dimensions of 2° and 40 mm in diameter. An amplitude sweep was performed to confirm that the frequency and strain were within the linear viscoelastic region.

To quantify the gelation temperature of materials, oscillation experiments were performed to measure the elastic modulus (G') and the viscous modulus (G'') as a function of temperature at a frequency of 1 Hz.

Temperature was increased at $1\,^{\circ}\text{C/min}$. The gelation point was the temperature at which G' equaled G''.

To measure the thixotropic loop of materials, flow experiments were performed to measure the viscosity as a function of shear stress [27]. Gels were equilibrated at $37\,^{\circ}\text{C}$ for 5 min, and the shear stress was swept from 10 to 300 Pa, and then swept from 300 to 10 Pa.

2.3. In vitro degradation

Degradations of 7% MC, 9% MC, HAMC, and acet-HAMC were performed in aCSF at $37\,^{\circ}\text{C}$ under agitation. Two ml eppendorf tubes filled with $900\,\mu\text{l}$ of aCSF were equilibrated to $37\,^{\circ}\text{C}$, and $100\,\mu\text{l}$ of the polymer solutions was injected into the bottom of the tubes ($n = 3$). The buffer was changed daily, and at 1, 4, 7, 14 and 28 d of incubation, the buffer was removed from the tubes, the polymer samples were lyophilized and degradation was quantified using the following equation:

$$\%\text{Degraded}(t) = \frac{(W_{\text{d}}(0) - W_{\text{d}}(t))}{W_{\text{d}}(0)}100, \qquad (1)$$

where $W_{\text{d}}(0)$ is the initial dry polymer mass and $W_{\text{d}}(t)$ is the dry polymer mass at time t.

2.4. Cell adhesion

3T3-NIH cells were cultured in DMEM media supplemented with L-glutamine, 10% fetal bovine serum, and 1% penicillin/streptomycin (pen/strep) in a $37\,^{\circ}\text{C}$, 5% CO_2 environment. To test for the cell adhesive properties of the gel, 50 mg of each gel material was dispensed in a 96-well plate in triplicate and incubated at $37\,^{\circ}\text{C}$ for 30 min. Two hundred microlitres of 3T3 cells in DMEM media (1×10^5 cells/ml) was added to the samples and incubated for 3 d. Collagen-coated wells were used as a positive control. An elongated cell morphology indicated that the material was adhesive, and cell clusters indicated that the material was non-cell adhesive ($n = 3$).

2.5. HAMC visualization in the intrathecal space

Fluorescent HA was synthesized by conjugating HA with BODIPY-FL hydrazide (Molecular Probes) using carbodiimide chemistry. To a 1% HA solution in ddH$_2$O, EDC was added in a 1:1 molar ratio to HA at pH 4–4.75, and BODIPY-FL hydrazide was added in a 1:4 molar ratio to HA at pH 2–4.75. The fluorescent HA solution was dialyzed and sterilized as described for unmodified HA. To make the fluorescent HAMC, the fluorescent HA accounted for 1% of the total HA in the blend.

The fluorescent gel was injected intrathecally in an uninjured rat as described in Section 2.6, and the cord was harvested fresh at 2 h, equilibrated in methyl-2-butane, flash frozen in dry ice, and sectioned parasagittally using a cryostat. Immediately thereafter, images were taken under a FITC filter using an upright microscope (Nikon) at a $10\times$ magnification, and tiled.

2.6. In vivo biocompatibility study

All animal procedures were performed in accordance with the Guide to the Care and Use of Experimental Animals (Canadian Council on Animal Care) and protocols were approved by the Animal Care Committee of the Research Institute of the University Health Network.

Twenty-four female Sprague Dawley rats (250–300 g; Charles River, Montreal, QC) were used to assess the effects of HAMC injected into the intrathecal space relative to aCSF in terms of animal function, histology and immunohistochemical responses. Four groups were compared: 4 uninjured animals were injected with $10\,\mu\text{l}$ of HAMC; 4 uninjured animals were injected with $10\,\mu\text{l}$ of aCSF (controls); 8 clip compression injured animals (35 g, 1 min, T2) were injected with $10\,\mu\text{l}$ of HAMC; and 8 clip compression injured animals (35 g, 1 min, T2) were injected with $10\,\mu\text{l}$ of aCSF (controls). The intrathecal injection method was fully described

previously by Jimenez-Hamann et al. [9]. Briefly, uninjured animals were anesthetized and subjected to a laminectomy at the T2 spinal level. The dura was punctured with a sharp 30G needle caudal to T2, and $10\,\mu\text{l}$ of sterile HAMC or aCSF was injected from a 1 ml Luer-loc syringe into the intrathecal space using a 30G, 22 mm-long anterior chamber cannula (Becton Dickinson & Company, Oakville, ON, CA). For injured animals, the identical procedure was followed except that animals had their spinal cords moderately injured prior to injection of the HAMC or aCSF. The spinal cord was moderately injured by cord compression with a 35 g modified aneurysm clip for 1 min utilizing techniques previously described from our laboratory [28]. After closing the overlying muscles, fascia and skin, rats were ventilated with pure oxygen and placed under a heating lamp for recovery. Animals were sacrificed 28 d after surgery and perfused intracardially with 10% neutral-buffered formalin. Spinal cords were harvested and post-fixed in formalin. Cords were then processed and embedded in paraffin blocks.

2.6.1. Histology

Two harvested cords of each of the 4 groups were cut parasagittally for qualitative observations, and the remaining were cut in 8 μm thick serial, transverse sections. Every 11th section was stained with Luxol Fast Blue, and counter-stained with hematoxylin and eosin (LFB/H&E). Slides were examined for general tissue morphology and cavity area. The cavity area was quantified on all sections stained with LFB/H&E over the entire cavity. Images were captured using bright-field microscopy (Olympus, BX61) at $1.25\times$ magnification, and analyzed with an image analysis system (Image Pro Plus; Media Cybernetics) that traced the cavitated region, and the spinal cord cross section. The total cavity volume was calculated using the Cavalieri method [29]. The % of lesion area was calculated as the area of the cavitated region divided by the total area of the spinal cord cross section.

2.6.2. Immunohistochemistry

The remaining sections were stained with anti-rat ED-1 (Serotec, Raleigh, NC) to examine for the presence of macrophages or Terminal Deoxynucleotidyltransferase-Mediated dUTP Nick End-Labeling (TUNEL) (ApopTag In Situ Apoptosis Detection kit, Chemicon International, Inc., Temecula, CA) to detect apoptotic cells following standard immunohistochemistry techniques, as previously described [30,31]. To quantify the inflammatory response and the number of apoptotic cells, 3 sections (-880, 0, and $+880\,\mu\text{m}$ relative to the lesion epicenter) of each animal were analyzed and averaged. Images of the sections were captured at $10\times$ magnification, and the area of the macrophages was determined based on the pixel intensity. To quantify the number of apoptotic cells, TUNEL positive cells were counted.

2.6.3. Functional analysis

Open-field motor function was evaluated using the Basso, Beattie and Bresnahan (BBB) scoring scale [32] at 4, 7, 14, 21, and 28 d after surgery. The scoring scale is a 21-point scale that ranks no locomotion as 0 points and normal gait as 21 points. Each hind limb was ranked by two blinded observers.

Limb placement and motor control was assessed by grid walk as described by Metz et al. [33]. Animals were trained to cross a grid walk for 5 d prior to surgery. After surgery, animals crossed the grid walk (1 m) at 7, 14, 21, and 28 d after injection. The number of foot falls that the rat made was counted.

2.7. Statistical analysis

All statistics were performed using SigmaStat 2.0. Student's t-test was used to compare the cavity area, inflammatory response, and number of apoptotic cells in injured animals. Mixed factorial ANOVA followed by the Bonferroni post-hoc t-test was used to compare BBB and grid walk scores of injured and uninjured animals [34]. Differences were accepted to be statistically significant at $p < 0.05$. All errors are given as standard deviations.

3. Results

The criteria for the injectable gel were fast-gelling, degradable, non-cell adhesive, and biocompatible within the intrathecal space. Each of these properties was analyzed as described below.

3.1. Gelation and rheology

The four gels, 7% MC, 9% MC, HAMC and acet-HAMC were tested for gelation by the inverted tube test and by rheology. By the inverted tube test, HAMC gelled fastest, taking less than 2 min to gel whereas 9% MC took 10 min, and 7% MC and acet-HAMC took 20 min. In the rheology study, G' and G'' were measured as a function of temperature and the point where G' equals G'' is known as the gelation temperature [35,36]. Interestingly, as shown in Fig. 1, the gelation point for HAMC (18 °C) is lower than that of 9% MC (27 °C), acet-HAMC (31 °C) and 7% MC (32 °C). The gelation point of HAMC indicates that it is a gel prior to injection in the intrathecal space and it is the shear-thinning properties of HA that allow it to be injected via syringe.

To investigate this shear-thinning property further, viscosity measurements were made at increasing and decreasing shear stress, producing the thixotropic loop of the material. The larger the area between the increasing and decreasing curves, the more time it takes for the material to recoil back to its original form. As shown in Fig. 2, in which the viscosity of the gel was measured as a function of shear stress, the area between the HAMC curves is smaller than those of acet-HAMC, 7% MC and 9% MC, qualitatively indicating that HAMC can recover from deformation much faster than 7% MC, 9% MC and acet-HAMC. These data reflect the shear-thinning and fast-gelling nature of HAMC after injection, further confirming the inverted test tube data.

3.2. In vitro degradation

To obviate the need for a second surgery to remove the gel after drug delivery, the injectable gel must be degradable. Fig. 3 shows the degradation profile of the four gels at 37 °C in buffer: 7% MC and HAMC are 90% degraded (or eroded) at 14 d whereas 9% MC and acet-HAMC are approximately 65% eroded at 14 d. The slower degradation profile for acet-HAMC, relative to HAMC, was expected due to the hydrophobic acetyl groups. Similarly, in 9% MC, more hydrophobic interactions are possible and result in slower dissolution. The combination of the fast-gelation measured by rheology and degradation properties of HAMC, led us to further characterize this gel for cell adhesion, ability to remain localized in vivo, and in vivo biocompatibility.

3.3. Cell adhesion

It is desirable for the injectable gel to be non-cell adhesive since an adhesive biomaterial could promote cell invasion within the matrix and scar formation within the
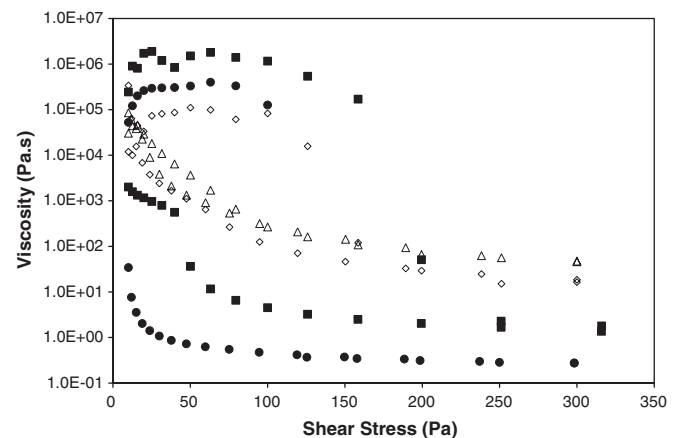
Fig. 2. Thixotropic loop of injectable gels at 37 °C (●) 7%MC, (■) 9%MC, (△) HAMC, and (◇) acet-HAMC.
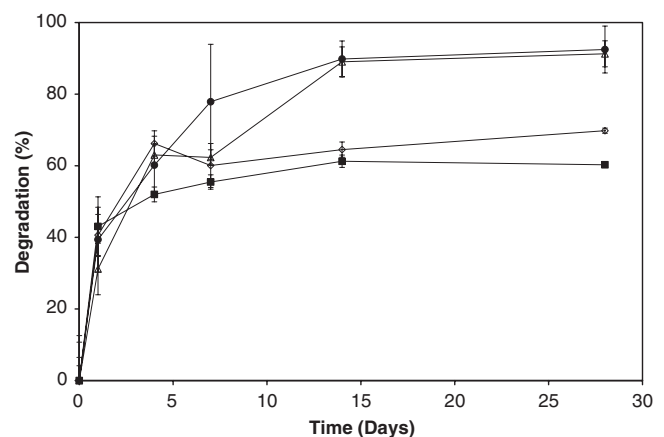
Fig. 3. In vitro degradation in aCSF of (●) 7%MC, (■) 9%MC, (△) HAMC, (◇) acet-HAMC determined by change of dry mass over time. Data are shown as mean ± standard deviation ($n = 3$).

Fig. 1. Elastic and viscous moduli of injectable gels at 1 Hz using a rheometer with a cone and plate geometry (●) 7%MC G', (○) 7%MC G'', (■) 9%MC G', (□) 9%MC G'', (▲) HAMC G', (△) HAMC G'', (◆) acet-HAMC G', and (◇) acet-HAMC G''.

intrathecal space, both of which would result in serious clinical complications [37–39]. To test for cell adhesion, 3T3 fibroblast cells were cultured on the gels, and the cell response was compared to positive collagen controls. Cell adhesion was qualitatively assessed in terms of cell clustering vs. cell spreading where the former indicates poor cell adhesion and the latter good cell adhesion. Cell adhesion to HAMC was minimal as cells adhered to each other and formed large cell clusters as opposed to adhering and spreading on the gel surface, as was observed for the collagen-coated control (data not shown). This indicates that the gel is non-adhesive to fibroblast cells, which suggests the potential for non-cell adhesion in vivo.

3.4. HAMC visualization in the intrathecal space

To facilitate visualization of the gel at the site of injection, fluorescent HAMC was injected into the intrathecal space. Fig. 4 shows fluorescent HAMC in the intrathecal space 2 h after injection demonstrating its utility for localized release.

3.5. In vivo biocompatibility

3.5.1. Histology and immunohistochemistry

HAMC was injected into the intrathecal space of clip compression-spinal cord injured and uninjured rats, and compared to the injection of aCSF for tissue morphology and function. Histological analysis through LFB/H&E of the uninjured (Figs. 5A, B) and injured (Figs. 5C, D) cords at 28 d shows that there were no observable differences between the HAMC-injected animals (Figs. 5B, D) and aCSF-injected controls (Figs. 5A, C). The dorsal surface of the spinal cords did not appear flattened indicating lack of compression from either the material or the injection technique. Moreover, scar formation, arachnoiditis and syringomyelia were not observed in either group. There was no evidence at 28 d that any of the HAMC had persisted in the intrathecal space.

It was observed in Figs. 5E and F that the dura resealed better in the HAMC-injected animals versus the aCSF-

injected controls at 1 month, because the dura in the HAMC-injected animals was completely sealed, and there was minimal arachnoidal cell reaction present. The resealed dura was thicker than the normal dura, but was composed of collagen (data not shown), similar to the normal dura. This re-sealing of the dura suggests some benefit of HAMC alone, in addition to being relatively inert, as compared to injection of aCSF controls.
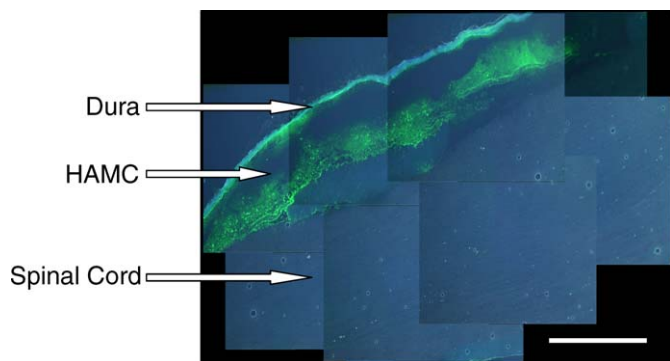
The cavitation volume and lesion epicenter area were determined using image analysis software. As shown in Table 1, the cavitation volume and lesion epicenter area are less for HAMC than aCSF, but not statistically different ($p = 0.10$). Quantification of apoptotic cells, in the lesion center and 880 μm rostral and caudal to the epicenter, was based on TUNEL staining, and also showed no significant differences between groups. This indicates that neither the injection method nor HAMC adversely affect the spinal cord and severity of injury.

ED-1 immunohistochemistry was used to stain for macrophages and microglia in the uninjured and injured spinal cord. In uninjured animals at 28 d, both HAMC- and aCSF-injected animals seemed to have similar, mild positive staining near the dura, as may be expected for any surgical intervention. Thus, HAMC did not cause a significant inflammatory reaction. In injured animals, the inflammatory response was quantified at the lesion epicenter and 880 μm rostral and caudal to the epicenter based on pixel intensity, and averaged. The HAMC-injected animals had significantly fewer inflammatory cells present at 28 d in comparison to aCSF-injected control animals (Table 1) based on the Student's t-test ($p = 0.04$).

3.5.2. Functional analysis

Function was assessed using BBB scoring and grid walk analysis. Fig. 6A shows BBB scores of injured and uninjured animals injected with either HAMC or aCSF over a period of 1 month. All the aCSF- and HAMC-injected uninjured animals had BBB scores of 21 throughout the study, indicating that neither the surgical technique nor HAMC affected the function of uninjured animals. While HAMC-injected injured animals had better BBB scores than the injured aCSF controls, only day 7 data were significantly different according to mixed factorial ANOVA, followed by the post-hoc Bonferroni t-test, $F(1, 14) = 7.58$, $p = 0.035$.

Grid walk measurements were performed weekly after surgery and are most useful as a predictor of motor function and coordination when animals have regained weight support. As shown in Fig. 6B, uninjured animals had nearly perfect scores of 0 foot falls throughout a run for both HAMC-and aCSF-injected animals, thereby corroborating the normal BBB scores described above for these groups (Fig. 6A). For injured animals, HAMC-injected animals had fewer foot falls than aCSF-injected controls, yet the difference between HAMC-injected and aCSF-injected animals was not statistically different as determined by mixed factorial ANOVA.

Fig. 4. Parasagittal section of rat spinal cord rostral to site of injection shows that the fluorescent HAMC is localized in situ in the intrathecal space where it was injected (scale bar = 1 mm).
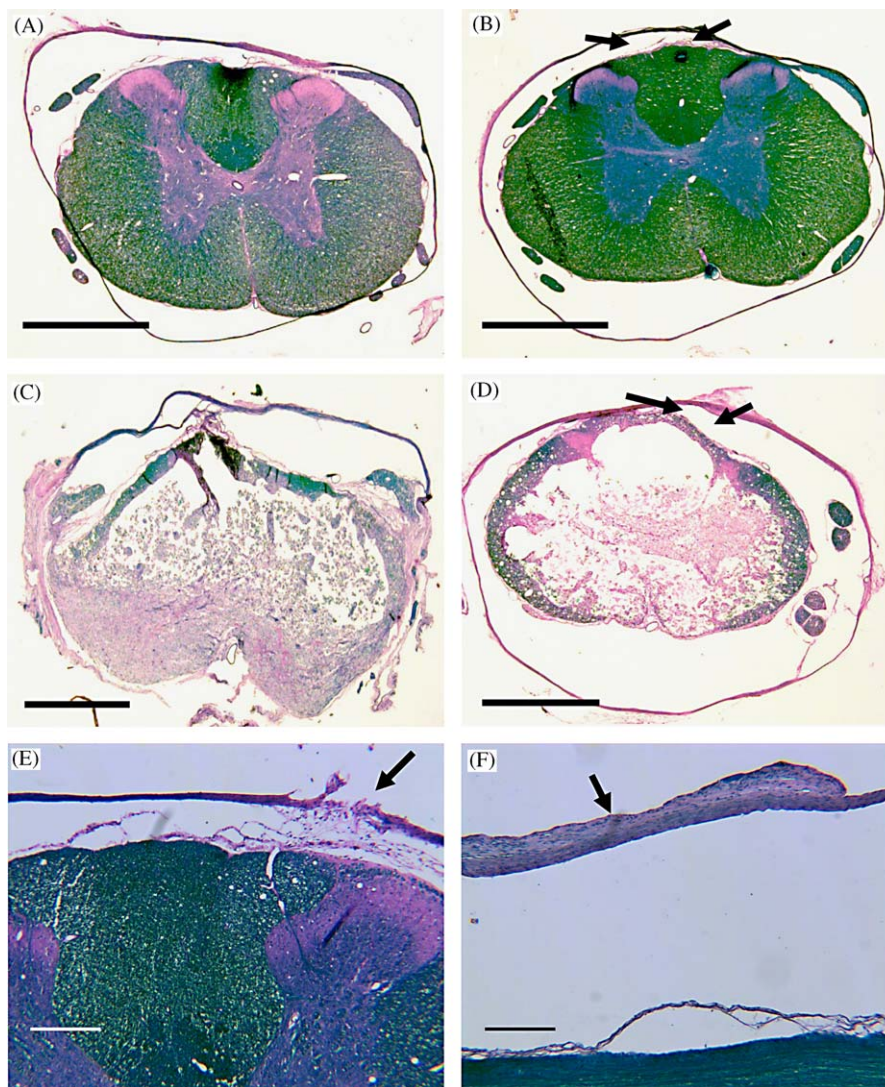
Fig. 5. Representative sections of each experimental group stained with Luxol Fast Blue and counterstained with hematoxylin and eosin: (A) uninjured rat injected with aCSF, (B) uninjured rat injected with HAMC. Arrows point to dorsal surface where HAMC was injected: (C) injured rat injected with aCSF, (D) injured rat injected with HAMC. Arrows point to dorsal surface where HAMC was injected (scale bar = 1 mm). (E&F) Sections showing injection site in dura of: (E) uninjured rat injected with aCSF (arrow points to unsealed dura that was punctured with needle) and (F) uninjured rat injected with HAMC (arrow points to resealed dura) (scale bar = 200 μm).

Table 1
Quantitative histological data comparing injection of aCSF and HAMC in injured animals in terms of lesion volume, area of lesion epicenter, quantification of ED-1 labelled macrophages/microglia based on pixel intensity and number of TUNEL positive apoptotic cells

	aCSF	HAMC
Cavity volume (mm^3)	52.1 ± 20.1	36.6 ± 6.0**
Lesion area at epicenter (%)	75.4 ± 8.6	71.5 ± 8.7
Number of apoptotic cells	38.8 ± 10.56	38.9 ± 7.99
Inflammatory cells (μm^2)	$3.79 \pm 1.39 \times 10^5$	$2.42 \pm 0.35 \times 10^5$ *

Data are shown as mean $\pm$ standard deviation ($n = 6$).
*The asterisk for inflammatory cells indicates significant difference ($p = 0.04$).
**$p = 0.10$.

4. Discussion

HAMC met our design criteria for fast gelation due to the fact that it both was a gel at room temperature prior to injection, as evidenced by the oscillatory rheology experiment, and had a quick re-coil back to a gel after shear, as evidenced by the flow experiment. Thus HAMC differs from other physical gelling polymers, including both 7% MC and 9% MC, which start as solutions and undergo a phase transition to gel after increase in temperature. Interestingly, acet-HAMC did not share the lower gelation temperature of HAMC, and this can be attributed to the acetyl groups present on acet-HA which block the activity of HA carboxylic acids that played an important role in

(A)

(B)
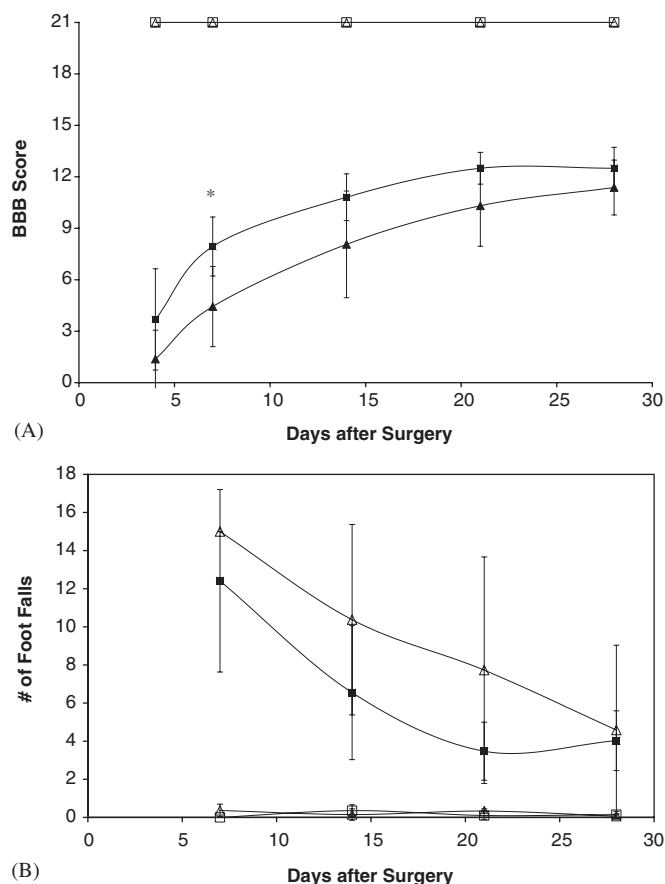
Fig. 6. (A) BBB scores over 28 days to measure the effect of HAMC on animal function: (□) HAMC uninjured, (△) aCSF uninjured, (■) HAMC injured, and (▲) aCSF injured. The two uninjured groups scored normal (21 points) at all times; (B) the number of foot falls per grid walk run for (□) HAMC uninjured, (△) aCSF uninjured, (■) HAMC injured and (▲) aCSF injured. The two uninjured groups had virtually zero footfalls at all times. Data are shown as mean ± standard deviation (uninjured animals: $n = 4$; injured animals $n = 8$). (*) at day 7 in (A) indicates significant difference ($p = 0.035$).

HAMC gelation (Fig. 1). As previously shown by Xu et al., the addition of anionic salts to MC decreases its gelation temperature [16] because the negative charges interact with the aqueous solvent, thereby dehydrating the MC chains. This dehydration effect results in MC polymers interacting less with the solvent and more with each other, thereby reducing the gelation temperature. The anionic carboxylic acid groups on HA act as anionic salts and have a similar effect on the surrounding solvent, likely resulting in the decreased gelation temperature of HAMC. The benefit of using HA instead of anionic salts to decrease the gelation temperature of MC is that the gel can retain its injectability due to the shear-thinning property of HA. Given that 80% of the carboxylic acids are acetylated in acet-HAMC, acet-HA had a less pronounced salting-out effect than was observed with HA, thereby explaining the difference in gelation temperature between HAMC and acet-HAMC. The difference in gelation temperature

between acet-HAMC and 9% MC indicates that the hydrophobic HA derivative did not aid in gel formation, as is seen when the MC concentration of the gel is increased.

Flow experiments on the rheometer indicate that HAMC is able to regain its initial viscosity faster than the other gels studied after an applied shear force, based on the areas of the thixotropic loops (Fig. 2). These results indicate that after injection, HAMC is able to recoil back to its gel-like structure faster than 7% MC, 9% MC and acet-HAMC, reflecting the shear-thinning properties of HA. The ability of HAMC to regain its high viscosity faster than MC is important for the in vivo application of localized drug delivery as it suggests that the HAMC will not flow away from the injection site prior to gelation (Fig. 4), or spread as far as MC would, under the CSF flow. The highly viscous nature of HAMC enhances the propensity for localized release into the spinal cord at the site of injection where the HAMC gel will strengthen with an increase in temperature. Thus, the fast-gelling property of HAMC is due to both the thermal gelling properties associated with MC (and enhanced by HA carboxylic acid salts) and the shear-thinning properties associated with HA.

To gain greater perspective on the degradation properties of HAMC, its degradation profile was compared to that of 7% MC, 9% MC and acet-HAMC in aCSF (Fig. 3). HAMC eroded at a similar rate to 7% MC and faster than both acet-HAMC and 9% MC. The increased hydrophobicity of HA derivatives is known to decrease water penetrability within the gel, thereby explaining the slower degradation observed for acet-HAMC versus HAMC. Similarly, 9% MC is known to erode slower than 7% MC simply due to the greater number of hydrophobic interactions associated with the higher-percent solids of MC. The similar degradation rate between the 7% MC and HAMC suggests that HAMC degradation is dominated by that of MC. Although HA influences gelation through the salting-out effect, HA is likely not involved in the hydrophobic interactions of MC. Thus HAMC eroded faster than 9% MC because degradation is dominated by the MC content which was 7% in HAMC. Acet-HAMC degraded slower than 7% MC (and only slightly faster than 9% MC), suggesting that acetyl groups increased the overall hydrophobicity of the gel, and thus affected water penetrability.

To assess the biocompatibility of HAMC, both tissue morphology and function were compared after injection of HAMC and aCSF in uninjured and moderately injured rats for one month. There was no evidence of cord compression or an increase in the severity of injury in either uninjured or injured animals. For injured animals, cavitation volume and area of lesion epicenter were not statistically different between the HAMC-injected and aCSF-injected controls. Moreover, no significant difference in the number of apoptotic cells between injured groups was observed. Collectively, these results indicate that

HAMC does not have an adverse effect on the spinal cord. In addition, the inflammatory response due to HAMC injection was minimal and less than aCSF injection in the injured animals at 28 d. In injured animals, macrophages/microglia were confined to the spinal cord tissue and were not observed surrounding the dura in either HAMC- or aCSF-injected animals. The decreased inflammatory response at 28 d observed after HAMC injection (relative to aCSF injection) may reflect the beneficial anti-inflammatory effects attributed to HA in other tissues [40–43]. The re-sealing of the dura (Figs. 5E, F) provides another advantage over other delivery techniques, such as bolus and intrathecal minipump where the dura may not seal at the punctured site, resulting in the potential for CSF leakage and/or infection.

The histology data were corroborated by the functional data showing that HAMC did not adversely affect the behavior of uninjured or injured animals relative to aCSF controls, as assessed by BBB and grid walk analysis. Uninjured animals were used to determine if HAMC itself or the method of injection (with injection of aCSF controls) caused deficits in fine motor function. All uninjured animals had BBB scores of 21 throughout the duration of the study with no significant difference from the aCSF controls, demonstrating that neither HAMC nor the injection method adversely affected motor function. While there was a trend for improved function in HAMC-injected injured animals compared with aCSF-injected injured controls, the data were not significantly different, except at 7 d, when the HAMC-injected animals had a higher BBB score than the aCSF-injected controls ($p = 0.035$). This potential benefit may reflect the decreased inflammatory response observed by immunohistochemistry.

The grid walk data corroborated the BBB scores, in which uninjured animals had essentially no foot falls after injection of either HAMC or aCSF. Unlike the BBB score system where a change in 1 or 2 points indicates a change in motor function, 1 or 2 foot falls on the grid walk are not indicative of such deficits. Normal rats making 1 or 2 foot falls per run have been reported by numerous groups [29,33] and are attributed to rats being more careless when walking across the grid faster. Thus it was expected that the uninjured animals in this study would not always achieve 0 foot falls during a grid walk test (Figs. 6B). The number of foot falls between the injured animal groups was not significantly different after injection of HAMC vs. aCSF. Unlike the BBB scoring system, the grid walk analysis did not show a statistical difference between HAMC- and aCSF-injected animals at 7 d, likely because of the greater variance observed with grid walk compared to BBB scoring. However, there was a trend for HAMC-injected animals to have fewer foot falls than aCSF controls.

Overall, the lower inflammatory response combined with the trend of improved functional behavior in the HAMC-injected animals relative to aCSF-injected controls over the entire month, and a statistically significant difference at 7 d in BBB scoring suggest that HAMC provides mild neuroprotection in the injured spinal cord [44]. Attenuation of free radicals at the injured site by antioxidants or anti-inflammatory agents provide neuroprotection and improved functional outcome [45,46]. Both HA and cellulose derivatives have antioxidant properties [47], and HA has previously been shown to have anti-inflammatory activity in vitro and in vivo [40–43]. Moreover, low molar mass HA is well-known for its inherent wound healing properties, such as promoting angiogenesis [48]. The mechanism of HAMC's potential benefit in the present study is unknown, but it is clear that HAMC provides an excellent vehicle for localized delivery of neuroprotective or neuroregenerative agents to be released within the first few days following injury. HAMC represents an improvement over our previous DDS that contained collagen. The advantages of HAMC are faster gelation for improved localized drug delivery; non-cell adhesive to minimize cellular build-up within the intrathecal space; and improved animal function relative to controls.

5. Conclusions

A new fast-gelling injectable gel was developed that involved blending shear-thinning HA with inverse thermal gelling MC to form HAMC. HAMC was a gel prior to injection and the gel strength increased after injection due to the increased temperature in the body relative to room temperature. The HAMC blend was found to have a lower gelation temperature and smaller thixotropic loop than MC alone and these effects were attributed to the anionic carboxylic acid salt groups of HA. In addition to being fast gelling, HAMC is non-cell adhesive, degradable, and biocompatible in the intrathecal space. In on-going studies, this promising gel is being investigated for the localized, sustained release and therapeutic benefit of bioactive molecules for the injured spinal cord.

References

[1] Ramer LM, Ramer MS, Steeves JD. Setting the stage for functional repair of spinal cord injuries: a cast of thousands. Spinal Cord 2005;43(3):134–61.

[2] Tsai EC, Dalton PD, Shoichet MS, Tator CH. Synthetic hydrogel guidance channels facilitate regeneration of adult rat brainstem motor axons after complete spinal cord transection. J Neurotrauma 2004;21(6):789–804.

[3] Pearse DD, Pereira FC, Marcillo AE, Bates ML, Berrocal YA, Filbin MT, et al. cAMP and Schwann cells promote axonal growth and functional recovery after spinal cord injury. Nat Med 2004;10(6): 610–6.

[4] Bracken MB, Shepard MJ, Holford TR, Leo-Summers L, Aldrich EF, Fazl M, et al. Methylprednisolone or tirilazad mesylate administration after acute spinal cord injury: 1-year follow up. Results of the third national acute spinal cord injury randomized controlled trial. J Neurosurg 1998;89(5):699–706.

[5] Gorio A, Gokmen N, Erbayraktar S, Yilmaz O, Madaschi L, Cichetti C, et al. Recombinant human erythropoietin counteracts secondary injury and markedly enhances neurological recovery from experimental spinal cord trauma. Proc Natl Acad Sci USA 2002;99(14): 9450–5.

[6] Terada H, Kazui T, Takinami M, Yamashita K, Washiyama N, Muhammad BA. Reduction of ischemic spinal cord injury by dextrorphan: comparison of several methods of administration. J Thorac Cardiovasc Surg 2001;122(5):979–85.

[7] Yaksh TL, Horais KA, Tozier N, Rathbun M, Richter P, Rossi S, et al. Intrathecal ketorolac in dogs and rats. Toxicol Sci 2004;80(2): 322–34.

[8] Jones LL, Tuszynski MH. Chronic intrathecal infusions after spinal cord injury cause scarring and compression. Microsc Res Tech 2001;54(5):317–24.

[9] Jimenez Hamann MC, Tsai EC, Tator CH, Shoichet MS. Novel intrathecal delivery system for treatment of spinal cord injury. Exp Neurol 2003;182(2):300–9.

[10] Jimenez Hamann MC, Tator CH, Shoichet MS. Injectable intrathecal delivery system for localized administration of EGF and FGF-2 to the injured rat spinal cord. Exp Neurol 2005;194(1):106–19.

[11] Jimenez Hamann MC. A novel strategy for localised delivery of therapeutic agents to the injured spinal cord [PhD]. Toronto: University of Toronto; 2003.

[12] Gutowska A, Jeong B, Jasionowski M. Injectable gels for tissue engineering. Anat Rec 2001;263(4):342–9.

[13] Hoffman AS. Hydrogels for biomedical applications. Adv Drug Deliv Rev 2002;54(1):3–12.

[14] Shu XZ, Ghosh K, Liu Y, Palumbo FS, Luo Y, Clark RA, et al. Attachment and spreading of fibroblasts on an RGD peptide-modified injectable hyaluronan hydrogel. J Biomed Mater Res A 2004;68(2):365–75.

[15] Li L, Thangamathesvaran PM, Yue CY, Tam KC, Hu X, Lam YC. Gel network structure of methylcellulose in water. Langmuir 2001;17(26):8062–8.

[16] Xu Y, Wang C, Tam KC, Li L. Salt-assisted and salt-suppressed sol–gel transitions of methylcellulose in water. Langmuir 2004;20(3): 646–52.

[17] Liang HF, Hong MH, Ho RM, Chung CK, Lin YH, Chen CH, et al. Novel method using a temperature-sensitive polymer (methylcellulose) to thermally gel aqueous alginate as a pH-sensitive hydrogel. Biomacromolecules 2004;5(5):1917–25.

[18] Hoenich NA, Woffindin C, Mathews JN, Vienken J. Biocompatibility of membranes used in the treatment of renal failure. Biomaterials 1995;16(8):587–92.

[19] Tate MC, Shear DA, Hoffman SW, Stein DG, LaPlaca MC. Biocompatibility of methylcellulose-based constructs designed for intracerebral gelation following experimental traumatic brain injury. Biomaterials 2001;22(10):1113–23.

[20] Wells MR, Kraus K, Batter DK, Blunt DG, Weremowitz J, Lynch SE, et al. Gel matrix vehicles for growth factor application in nerve gap injuries repaired with tubes: a comparison of biomatrix, collagen, and methylcellulose. Exp Neurol 1997;146(2):395–402.

[21] Vercruysse KP, Prestwich GD. Hyaluronate derivatives in drug delivery. Crit Rev Ther Drug Carrier Syst 1998;15(5):513–55.

[22] Balazs EA. Medical applications of hyaluronan and its derivatives. In: Gebelein CG, editor. Cosmetic and pharmaceutical applications of polymers. New York: Plenum Press; 1991. p. 293–310.

[23] Moriyama K, Ooya T, Yui N. Hyaluronic acid grafted with poly(ethylene glycol) as a novel peptide formulation. J Control Rel 1999;59(1):77–86.

[24] Weiss C. Why viscoelasticity is important for the medical uses of hyaluronan and Hylans. In: Weigel GAaPH, editor. New frontiers in medical sciences: redefining hyaluronan: Excerpta Medica; 2000. p. 89.

[25] Barbucci R, Lamponi S, Borzacchiello A, Ambrosio L, Fini M, Torricelli P, et al. Hyaluronic acid hydrogel in the treatment of osteoarthritis. Biomaterials 2002;23(23):4503–13.

[26] Prestwich GD, Marecak DM, Marecek JF, Vercruysse KP, Ziebell MR. Controlled chemical modification of hyaluronic acid: synthesis, applications, and biodegradation of hydrazide derivatives. J Control Rel 1998;53(1–3):93–103.

[27] Herh P, Tkachuk J, Wu S, Bernzen M, Rudolph B. The rheology of pharmaceutical and cosmetic semisolids. Am Lab 1998:12–4.

[28] Rivlin AS, Tator CH. Effect of duration of acute spinal cord compression in a new acute cord injury model in the rat. Surg Neurol 1978;10(1):38–43.

[29] Hains BC, Saab CY, Lo AC, Waxman SG. Sodium channel blockade with phenytoin protects spinal cord axons, enhances axonal conduction, and improves functional motor recovery after contusion SCI. Exp Neurol 2004;188(2):365–77.

[30] Popovich PG, van Rooijen N, Hickey WF, Preidis G, McGaughy V. Hematogenous macrophages express CD8 and distribute to regions of lesion cavitation after spinal cord injury. Exp Neurol 2003;182(2): 275–87.

[31] Mizumatsu S, Monje ML, Morhardt DR, Rola R, Palmer TD, Fike JR. Extreme sensitivity of adult neurogenesis to low doses of X-irradiation. Cancer Res 2003;63(14):4021–7.

[32] Basso DM, Beattie MS, Bresnahan JC. Graded histological and locomotor outcomes after spinal cord contusion using the NYU weight-drop device versus transection. Exp Neurol 1996;139(2): 244–56.

[33] Metz GA, Merkler D, Dietz V, Schwab ME, Fouad K. Efficient testing of motor function in spinal cord injured rats. Brain Res 2000;883(2):165–77.

[34] Scheff SW, Saucier DA, Cain ME. A statistical method for analyzing rating scale data: the BBB locomotor score. J Neurotrauma 2002;19(10):1251–60.

[35] Elbert DL, Pratt AB, Lutolf MP, Halstenberg S, Hubbell JA. Protein delivery from materials formed by self-selective conjugate addition reactions. J Control Rel 2001;76(1–2):11–25.

[36] Winter HH, Chambon F. Analysis of linear viscoelasticity of a cross-linking polymer at the gel point. J Rheol 1986;30(2):367–82.

[37] Hamada Y, Ikata T, Katoh S, Katoh K, Niwa M, Tsutsumishita Y, et al. Effects of exogenous transforming growth factor-beta 1 on spinal cord injury in rats. Neurosci Lett 1996;203(2):97–100.

[38] de Vries J, Menovsky T, van Gulik S, Wesseling P. Histological effects of fibrin glue on nervous tissue: a safety study in rats. Surg Neurol 2002;57(6):415–22 (discussion 422).

[39] Sarwal V, Suri RK, Sharma OP, Baruah A, Singhi P, Gill S, et al. Traumatic subarachnoid-pleural fistula. Ann Thorac Surg 1996;62(6): 1622–6.

[40] Sheehan KM, DeLott LB, Day SM, DeHeer DH. Hyalgan has a dose-dependent differential effect on macrophage proliferation and cell death. J Orthop Res 2003;21(4):744–51.

[41] Dougados M. Sodium hyaluronate therapy in osteoarthritis: arguments for a potential beneficial structural effect. Semin Arthritis Rheum 2000;30(2, Suppl 1):19–25.

[42] Roth A, Mollenhauer J, Wagner A, Fuhrmann R, Straub A, Venbrocks RA, et al. Intra-articular injections of high-molecular-weight hyaluronic acid have biphasic effects on joint inflammation and destruction in rat antigen-induced arthritis. Arthritis Res Ther 2005;7(3):R677–86.

[43] Cabrera PV, Blanco G, Alaniz L, Greczanik S, Garcia M, Alvarez E, et al. CD44 and hyaluronic acid regulate in vivo iNOS expression and

metalloproteinase activity in murine air-pouch inflammation. Inflamm Res 2004;53(10):556–66.

[44] Rabchevsky AG, Fugaccia I, Fletcher-Turner A, Blades DA, Mattson MP, Scheff SW. Basic fibroblast growth factor (bFGF) enhances tissue sparing and functional recovery following moderate spinal cord injury. J Neurotrauma 1999;16(9):817–30.

[45] Hillard VH, Peng H, Zhang Y, Das K, Murali R, Etlinger JD, et al. Tempol, a nitroxide antioxidant, improves locomotor and histological outcomes after spinal cord contusion in rats. J Neurotrauma 2004;21(10):1405–14.

[46] Wells JE, Hurlbert RJ, Fehlings MG, Yong VW. Neuroprotection by minocycline facilitates significant recovery from spinal cord injury in mice. Brain 2003;126(Pt 7):1628–37.

[47] Moseley R, Leaver M, Walker M, Waddington RJ, Parsons D, Chen WY, et al. Comparison of the antioxidant properties of HYAFF-11p75, AQUACEL and hyaluronan towards reactive oxygen species in vitro. Biomaterials 2002;23(10):2255–64.

[48] Chen WY, Abatangelo G. Functions of hyaluronan in wound repair. Wound Repair Regen 1999;7(2):79–89.